Model-Based Dispatch Strategies for Lithium-Ion Battery Energy Storage Applied to Pay-as-Bid Markets for Secondary Reserve

Christoph Goebel, *Member, IEEE*, Holger Hesse, Michael Schimpe, Andreas Jossen, and Hans-Arno Jacobsen, *Senior Member, IEEE*

***Abstract*—Due to their decreasing cost, lithium-ion batteries (LiB) are becoming increasingly attractive for grid-scale applications. In this paper, we investigate the use of LiB for providing secondary reserve and show how the achieved cost savings could be increased by using model-based optimization techniques. In particular, we compare a maximum use dispatch strategy with two different cost-minimizing strategies. For the estimation of state-dependent battery usage cost, we combine an existing electro-thermal LiB model of a mature lithium-iron-phosphate battery cell with corresponding semiempirical calendar and cycle aging models. We estimate the benefit of storage operation from the system operator's point of view by gauging the avoided cost of activated reserve. Our evaluation is based on two years worth of data from the German reserve market. The proposed cost minimizing dispatch strategies yield significantly better results than a dispatch strategy that maximizes battery utilization.**

***Index Terms*—Ancillary services, battery aging, economic value, lithium-ion batteries, optimization.**

NOMENCLATURE

β_i	Battery model constants.
CAP_c	Nominal cell energy capacity [Ah].
c	Variable to denote cost.
c_c	Cost per battery cell [EUR].
c_b	Total BES cell cost [EUR/kWh].
d	Variable to denote time duration [h].
d_c	Duration of dispatch interval [h].
d_{cal}	Duration until given battery capacity fade [h].
η	Power electronics efficiency [frac.].
E_c	Nominal energy capacity of one cell [Wh].
E_b	Nominal BES energy capacity [MWh].
f_{cal}	Capacity fade resulting from calendar aging [frac].
f_{cyc}	Capacity fade resulting from cycle aging [frac].
f_{EOL}	Cell decommissioning capacity fade [frac].
f_t	Capacity fade of cell at time t [frac].
γ	Month to hours factor.
I	Cell current [A].
k	Variable to control time resolution (Fig. 3).
κ_T	Summand for °C to °K conversion.
n	Number of battery cells.
p	Variable to denote power.
$p_{\min}$	Minimum available BES power [MW].
$p_{\max}$	Maximum available BES power [MW].
$p_{r,t}$	Demand for reserve during dispatch interval t [MW].
$p_{r,t}^{\min}$	Minimum demand for reserve during dispatch interval t [MW].
$p_{r,t}^{\max}$	Maximum demand for reserve during dispatch interval t [MW].
p_t	BES dispatch during time interval t [MW].
$\mathfrak{P}_{r,t}^{\text{neg}}(.)$	Marginal negative reserve energy price during time interval t [EUR/MWh].
$\mathfrak{P}_{r,t}^{pos}(.)$	Marginal positive reserve energy price during time interval t [EUR/MWh].
Π	Cost savings resulting from BES dispatch [EUR].
$\phi(.)$	Probability density function of reserve demand.
Q	Heat generation inside cell [W].
r_c	C-rate.
R_{gas}	Gas constant.
$\mathfrak{R}$	Cost savings resulting from BES dispatch [EUR].
$\mathbf{S}$	Cell state as tuple $[f, SOC, T_c, T_s]$.
SOC	Storage/cell state of charge [frac.].
$SOC_{\min}$	Minimum storage/cell state of charge [frac.].
$SOC_{\max}$	Maximum storage/cell state of charge [frac.].
t	Start time of dispatch interval (also used as index).
T	Variable to denote temperature [°C].
T_c	Cell core temperature [V].
T_f	Surrounding temperature [°C].
T_m	Average of cell core and surface temperature [°C].
T_s	Cell surface temperature [°C].
u	Loss of life fraction.
V_{OCV}	Open circuit cell voltage [V].
V_{drop}	Voltage drop inside cell [V].

Manuscript received February 5, 2016; revised May 31, 2016 and September 6, 2016; accepted October 28, 2016. Date of publication November 8, 2016; date of current version June 16, 2017. This work was supported in part by the Alexander von Humboldt foundation. Paper no. TPWRS-00197-2016.

The authors are with Technical University Munich, Munich 80333, Germany (e-mail: goebelc@gmail.com; holger.hesse@tum.de; michael.schimpe@tum.de; andreas.jossen@tum.de; jacobsen@in.tum.de)

Digital Object Identifier 10.1109/TPWRS.2016.2626392

I. INTRODUCTION

THE integration of high shares of intermittent renewable energy sources results in new challenges for power system operators, who are in charge of maintaining a secure operating state of the power grid. Ancillary services, which system op-

erators use to ensure that supply matches demand at all times, become increasingly important. These services can be offered by fast-ramping generators that burn fossil fuels or by pumped hydro energy storage that depend on specific geographical features. However, several other types of energy storage systems are technically mature and able to provide ancillary services [1], [2], in particular battery energy storage (BES). BES can be sized for individual needs and integrated into existing low and mid voltage grids. Power electronics for battery control may react very fast to control active and reactive power injection. Although still relatively expensive today, system operators are starting to deploy lithium-ion batteries (LiBs) for grid-scale energy storage [3]. Compared to most other types of commercially mature electrochemical energy storage technologies, LiBs have very high energy density, reach high round-trip efficiencies, and have long cycle lives. Furthermore, a rapid cost decline is anticipated for Li-Ion energy storage [4].

The aging behavior of chemical batteries such as LiBs, and therefore their variable usage costs, strongly depend on the way they are operated. Thus, for a profitable usage of LiBs and acceleration of their market adoption, "intelligent" LiB dispatch strategies should be developed that consider profit or overall cost savings as their main objective. Such operational strategies must be based on battery models that capture all relevant dynamics, in particular the capacity fade resulting from cell aging. The more accurate such models are, the greater are the potential financial advantages that can be realized if they are used to inform BES dispatch. In this paper, we propose methods that allow system operators to dispatch BES consisting of LiBs based on current battery and system conditions.

We address these research needs as follows:

1) We combine a state-of-the-art electro-thermal LiB cell model with semi-empirical calendar and cycle aging models.
2) We derive a model of state/action-based battery financial usage cost.
3) We propose two cost-based storage dispatch strategies and define a corresponding benchmark dispatch strategy that maximizes battery usage.
4) We demonstrate and compare the proposed dispatch strategies using German reserve market data.

This paper is organized as follows: In Section II, we review the related literature. Section III provides details on the battery model we use. In Section IV, we propose several control strategies for providing reserve energy. Section V describes the setup and results of a simulation study evaluating the cost savings resulting from the use of lithium-ion batteries for providing secondary reserve. Section VI discusses assumptions, limitations, and future work. Section VII provides final conclusions.

II. Related Work

Due to its key role in the transition to renewable energy, grid-scale energy storage is a very active research area. Chemical batteries are just one type of energy storage within a large spectrum of potential solutions [5]. Regarding the optimal operation of chemical batteries, the existing research can be divided into several categories based on the considered use case, which in turn influences the choice of battery models and optimization methods. The following use case attributes help to categorize research papers:

1) *Stakeholder* operating BES (e.g., utility, household, system operator)
2) *Purpose* of BES, i.e., how does the stakeholder achieve a benefit (e.g., energy market arbitrage, provision of ancillary services, locally balancing renewable output, peak-shaving)
3) *Type* of BES, i.e., what type of battery chemistry is considered (e.g., lead-acid, different lithium ion battery chemistries).

The approach described in this paper assumes that BES is controlled by the system operator. The purpose of the BES is to provide secondary reserve, a type of ancillary service, in the most financially efficient way. In contrast to energy market prices, the demand for ancillary services is too variable and uncertain for meaningful point predictions, which has important implications regarding the spectrum of applicable optimization techniques. We consider lithium-ion batteries, in particular lithium iron phosphate (LFP) cells, which are preferably used in stationary applications due to their properties (less energy density, but longer lifetime). Our use of a highly detailed electro-thermal battery behavior model with semi-empirical calendar and cycle aging models allows us to derive variable battery usage cost.

Many research papers analyze the contribution of energy storage in contexts that allow for predicting relevant environmental variables, including [6]–[13]. Although all cited papers consider batteries, they employ less detail battery models compared to our paper. These models typically allow for defining a few basic parameters that are treated as constants, in particular power and energy capacity, efficiency, and life time. The use of basic battery models facilitates the integration of energy storage into dispatch optimization models commonly used in the power systems community. However, it also limits the possibility of considering the variable cost of using batteries.

The work described in [6] investigates optimal BES operation when taking part in the Californian day-ahead and real-time *energy markets*. It takes the perspective of regular market participants, e.g., utilities, whereas our paper assumes that BES is operated by the system operator. Moreover, in contrast to our paper, [6] focuses on optimal storage dispatch based on energy market prices, for which a stochastic mixed integer linear optimization model is developed. The approach requires a linear energy storage model, which is less detailed compared to the model we use.

In [7], energy storage operation is integrated into a stochastic unit commitment model, which can be used to minimize total cost from the system operator's point of view. Their work, similar to [6], also focuses on day-ahead and intra-day *energy markets* using a basic model of battery energy storage. Thus, [7] differs from our paper with respect to all use case attributes except optimization perspective.

Reference [8] investigates another promising BES purpose, namely optimal co-dispatch of BES and conventional power plants trading off BES usage costs and ramping costs. They

develop a battery usage cost model based on storage cycles and depth of discharge, but do not employ a battery behavior model. In addition to generators and BES, they also consider transmission network constraints derived from a 118-bus IEEE system. They solve the resulting unit commitment problem to evaluate the financial impact of different BES sizes.

The approach presented in [9] is based on a battery behavior model. The model is used to determine optimal BES dispatch for energy market arbitrage. Similar to our paper, [9] models profit explicitly. However, the behavior model in [9] is only used to derive feasible power based on SOC, not to derive the variable and state-dependent cost of dispatch.

In [10], a method for optimal scheduling of electric vehicle (EV) charging and vehicle-to-grid services is proposed. The semi-empirical battery aging functions proposed in this work are comparable to ours, but the employed behavioral model is less detailed so that it can be integrated into a robust optimization framework to minimize EV charging cost.

In [11], a dynamic programming approach to dispatch batteries in combination with solar PV in a household setting is proposed. The approach is based on a behavioral battery capability model, coupled with a calendar aging model to consider a lifetime maximizing objective. They demonstrate their approach assuming perfect predictions of solar power production and household demand. Thus, although they use detailed battery models, they assume a predictable environment, which allows them to apply dynamic programming.

In [12], a variable cost model for lithium-ion battery usage is developed. This model is applied in a peak-shaving application. Similar to [13], [12] employs MPC to optimally dispatch the considered BES. To apply MPC, [12] derives independent linear or quadratic terms for the different components of battery wear they model, i.e., degradation caused by depth of discharge, power, and SOC. Our approach differs firstly with respect to the thermal component of the battery model we use, which allows us to use temperature-dependent aging models. Secondly, we consider the provision of secondary reserve, which defies the assumption of predictability required by MPC.

The approach described in [13] is based on a model of a lead-acid battery derived from an equivalent circuit. It employs model predictive control (MPC) relying on wind power forecasts that penalizes deviations from a reference (dis)charging power and limits SOC to a range between 30 and 100%, which is supposed to limit battery wear. In contrast to our paper, [13] does not specify explicit aging models or explicit profit maximization goals for their controller. Furthermore, perfect predictions of next-minute wind power generation and almost perfect predictions for the next hour are assumed.

Ancillary service provision differs from the use cases described above because their actual utilization is unpredictable. Several papers investigate the use of battery energy storage (BES) for providing ancillary services in power systems [14], [1], [15], [16], [17].

In [14], algorithms for scheduling large numbers of stationary batteries for providing reserve are proposed. It takes a market participant perspective. The employed battery model is based on actual measurements, but simplified to a linear approximation, similar to [6], [8]. The focus of [14] is clearly on the scalability of systems dispatching many batteries in accordance with strict market rules, not so much on leveraging accurate battery models to achieve higher cost savings or profits.

In [1], BES capacity size requirements for providing primary and secondary reserve are investigated. The presented approach employs set-point-based dispatch strategies which control a target state of charge (SOC) to minimize storage size. In contrast to our paper, [1] neither considers explicit maximization of cost savings, nor introduces detailed energy storage models.

Reference [15] investigates the profitability of sodium sulfur (NaS) based BES for providing ancillary services in California. It neither models battery behavior on the electrical or thermal level, nor proposes optimal dispatch strategies. However, it provides a highly interesting sensitivity study revealing the impact of different BES configurations (depth of discharge limits, power vs. energy rating) and compensation schemes (capacity vs. energy based compensation) on NaS profitability.

In [17], a method for dimensioning BES for the provision of primary reserve based on net present value (NPV) of BES investment is presented. Since primary control reserve is compensated based on capacity only, profit maximization translates to capacity minimization. Thus, although the paper focuses on ancillary services like ours, they do not use detailed battery behavior and aging models. Instead, the authors assume a fixed number of available cycles, which has the advantage of broader applicability in terms of battery types.

Similar to [17], [16] proposes a method for sizing the energy storage, but does not consider a detailed battery model or financial aspects. The work presented in [16] extends [17] to closed-loop control within an isolated power system. To enable the corresponding dynamic stability study, it employs an equivalent circuit model, first introduced in [18], to model battery voltage behavior.

In summary, the work presented in this paper is a unique contribution considering the current literature reviewed above. On the one hand, in contrast to other work focusing on ancillary services, we follow a cost savings maximization approach based on state-dependent, variable dispatch cost derived from comprehensive battery behavior (current, voltage, SOC, and temperature) and aging models (calendar and cycle aging). Variable dispatch cost is only applied by the authors of [12], but they do not link it to profit and their battery model is less detailed. Whereas some of the related papers do maximize cost savings or profit explicitly [9], [15], they use even more simplified battery cost models that do not consider detailed battery behavior. On the other hand, due to the impossibility to predict reserve utilization even for short-time horizons, MPC-based dispatch methods are not applicable to our use case. We therefore propose an alternative dispatch method that considers expected cost savings based on probability distributions of required reserve power.

III. Lithium-Ion Battery Model

Sections III-A and III-B contain descriptions of models provided in the literature, which we combine to obtain the variable cost model presented in Section III-C.

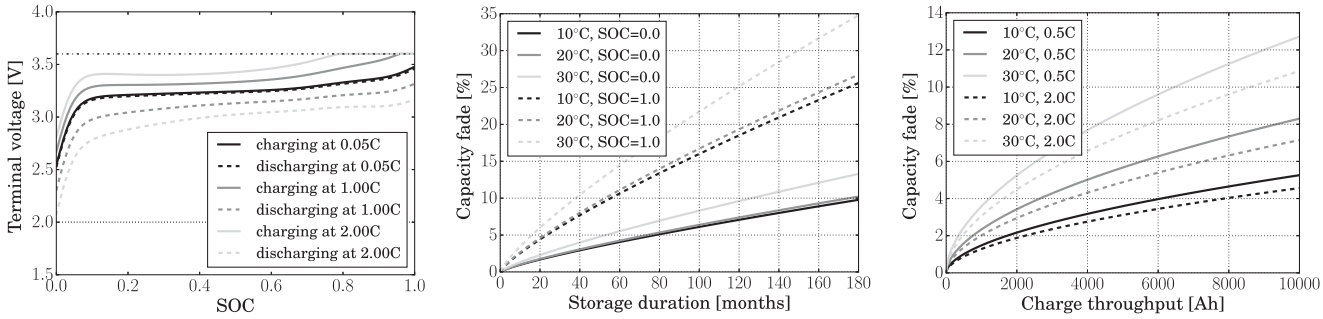

Fig. 1. Model demonstration. (a) Terminal voltage vs. SOC at $T = 20\ ^{\circ}\mathrm{C}$. (b) Storage capacity loss at different temperatures. (c) Cycling capacity loss at different temperatures.

A. Electro-Thermal Battery Cell Model

We apply the electro-thermal battery cell model described in [19], which mimics the behavior of an A123 ANR26650 lithium iron phosphate (LFP) battery cell. This cell type has a nominal capacity of $CAP_c = 2.3$ Ah, a *minimal* terminal voltage of 2.0 V, a *nominal* terminal voltage of 3.3 V, and a *maximum* terminal voltage of 3.6 V.

The model has two components: An equivalent circuit model describing the cell's terminal voltage, and a thermal model describing the evolution of temperature on the cell surface and in the cell's core. The equivalent circuit model is an OCV-R-RC-RC model, i.e., it consists of one series resistance and two resistance-capacitance parallel elements. According to [19], this type of circuit strikes an acceptable balance between model fidelity and complexity. Fig. 1(a) shows the terminal voltages resulting from different charging rates and SOC levels at constant currents according to the used model. As can be seen from the figure, the rate capacity effect, i.e., reduced efficiency at higher C-rates [20], is well captured. The thermal model is a two-state model, i.e., it describes the heat transfer between the cell's surroundings, the cell surface, and the cell core using two thermal resistances. Both models are coupled via the mutual influences of temperature on voltage and of current on temperature. In each simulation step, the cell model computes a new state based on the differential equations provided in [19]. To compute the next cell state, the cell current I and the surrounding temperature T_f need to be defined. Changes of the aging dependent relative state-of-charge are computed based on current integration (i.e., coulomb counting) according to Eq. 1. In Eq. 1, SOC denotes state of charge, d is a variable time duration, CAP_c denotes nominal cell capacity, and f_t is the capacity fade at time t in percent.

$$SOC(t+d) = SOC - \frac{I \cdot d}{CAP_c \cdot (1 - (f_t/100))} \qquad (1)$$

Terminal voltage results from the difference between the SOC-dependent open-circuit voltage V_{OCV} and the temperature-, current-, and SOC-dependent internal voltage drop V_{drop}, i.e., $V_t = V_{OCV} - V_{\mathrm{drop}}$. The heat generation Q inside the battery cell can be computed as the product of current and voltage drop, i.e., $Q = I \cdot V_{\mathrm{drop}}$. The authors of [19] do not provide a function of $V_{OCV}(SOC)$, therefore, we use the one provided in [21], which has been fitted to actual measurements of the same type of battery cell. The electro-thermal coupling is achieved by exchanging Q and $T_m = (T_s + T_c)/2$ between the electric and thermal model.

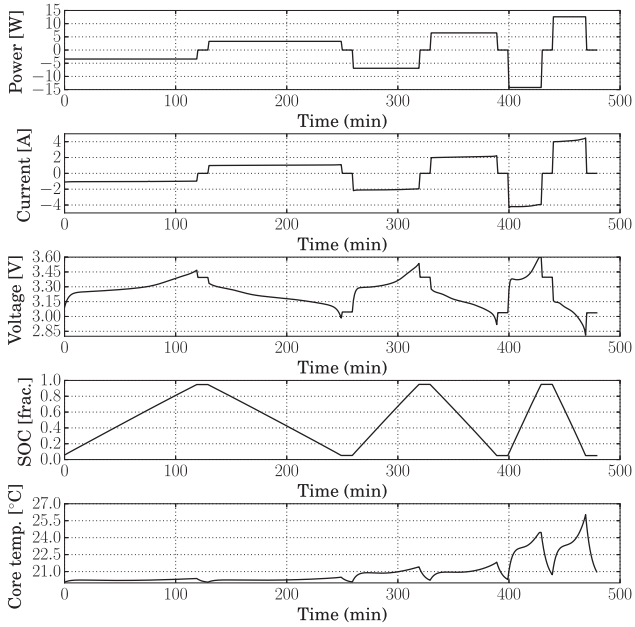

Fig. 2. Simulation results of the electro-thermal cell model with test cycles at increasing (dis) charging power levels.

We denote the function describing the cell state evolution by $nextState_I(\mathbf{S}, I, d)$, where the cell state $\mathbf{S}$ is defined as a value tuple consisting of the cell's current capacity fade f, the state of charge SOC, its core temperature T_c, and its surface temperature T_s, i.e., $\mathbf{S} = [f, SOC, T_c, T_s]$. The function $nextState_I$ then takes an initial state as input and updates it based on the applied current I during time duration d. We have chosen 1 s time resolution to allow for accurate SOC determination at each time step. Fig. 2 shows simulation results for terminal voltage, SOC and cell core temperature when charging and discharging at different C-rates.

To achieve constant power in- or output over an extended period of time, the cell current has to be modulated accordingly. For this purpose, we have developed a fast search algorithm (later denoted by $getI$) that takes the desired power p, as well as

the current SOC and mean temperature T_m as input, and returns the required current value. The simulation test results provided in Fig. 2 were obtained as output of our simulation program. They show power, current, terminal voltage, SOC, and core temperature of the simulated cell when charging and discharging at the maximum constant power for 120, 60, and 30 minutes, respectively, with a 10 minutes long rest period in between. The chosen (dis)charging duration approximately translate to C-rates of 0.5, 1, and 2, respectively. One can observe the energy loss due to cell efficiency considering the power levels, the impact of current modulation, as well as the rising and falling core temperature levels, depending on whether the battery is cycled or resting. Since the cell is cycled within a SOC range between 0.05 and 0.95 where it has a relatively constant terminal voltage (cf. Fig. 2), the current does not have to be strongly modulated to achieve constant power. The cell temperature usually decreases back to the surrounding temperature within 10 minutes, even at the highest C-rates considered in this study.

B. Lifetime Model for Battery Cell

Two main factors contribute to the aging of lithium-ion batteries: calendar and cycle aging. Calendar aging refers to the irreversible loss of capacity during storage, i.e., when the battery is not (dis)charged. Cycle aging refers to the capacity loss when the battery is actively charged or discharged. The aging of commercial lithium-ion cells, like the one we consider in this study, is usually investigated based on accelerated lifetime tests. We did not carry out such test ourselves, but use corresponding semi-empirical models available in the literature instead.

$$f_{cal}(d, T_s, SOC) = \ (\beta_1 \cdot SOC^{\beta_2} + \beta_3) \cdot (\beta_4 \cdot T_s^{\beta_5} + \beta_6) \cdot d^{\beta_7} \tag{2}$$

Eq. 2 is a function that was fitted to measurements of capacity fade of stored battery cells of the investigated type in [22]. The variable f denotes capacity fade (measured in percent). The fitted parameters are $\beta_1 = 0.019$, $\beta_2 = 0.823$, $\beta_3 = 0.5195$, $\beta_4 = 3.258 \times 10^{-9}$, $\beta_5 = 5.087$, $\beta_6 = 0.295$, and $\beta_7 = 0.8$. The duration d provided as input to Eq. 2 is measured in months, the required storage temperature T_s in degrees Celsius, and the SOC as percentage. Based on Eq. 2, the duration until a certain capacity fade has been reached can be expressed by Eq. 3.

$$d_{cal}(f, T_s, SOC) = \\ (f/((\beta_1 \cdot SOC^{\beta_2} + \beta_3)(\beta_4 \cdot T_s^{\beta_5} + \beta_6)))^{1/\beta_7} \tag{3}$$

Eq. 4 represents an approximation of capacity fade (measured in percent of the nominal capacity) when the battery is cycled, i.e., if the cell current deviates from zero. This power law-based expression of capacity fade depending on battery capacity throughput measured in Ampere hours (Ah) was first introduced in [23]. The authors of [23] also showed that depth of discharge has a negligible effect on battery life when considering charge throughput instead of (dis)charging cycles. The surface temperature T_s provided as input to function f_{cyc} is measured in degrees Celsius, with κ_T denoting the conversion summand to degrees Kelvin, i.e., $\kappa_T \approx 273.15$. R_{gas} is the gas constant, i.e., approximately equal to 8.31446. The variable r_c is the C-rate at which the cell was cycled during the tests.

```
1: Input: S, p, d
2: u ← 0
3: for t = 1 → k · d do
4:     u_cal ← 1/(k·d) · [γ · d_cal(f_EOL, S.T_s + κ_T, S.SOC)]^{-1}
5:     if p = 0 then
6:         u ← u + u_cal
7:     else
8:         I ← getI(S, p)
9:         if |I| > r_c · CAP_c then
10:            return u ← ∞
11:        r_c ← max{min{|I|/CAP_c, 2}, 0.5}
12:        u_cyc ← [k/|I| · Ah_cyc(f_EOL, S.T_s + γ_2, r_c)]^{-1}
13:        u ← u + max{u_cal, u_cyc}
14:    S ← nextState_I(S, I, d/k)
15:    if S.SOC < SOC_min or S.SOC > SOC_max then
16:        return u ← ∞
17: return u
```

Fig. 3. Algorithm for computing value of $u(\mathbf{S}, p, d)$.

$$f_{cyc}(Ah, T_s, r_c) = \\ \beta_8(r_c) \cdot \exp(\beta_9(r_c)/(R_{gas} \cdot (T_s + \kappa_T)))(0.5 \cdot Ah)^{\beta_{10}} \tag{4}$$

The fitted variables in Eq. 4 are $\beta_8(r_c) = 31,630 - (2 \cdot r_c/3 - 1/3) \cdot 9,949$, $\beta_9(C) = 370.3 \cdot r_c - 31,700$, with $r_c \in [0.5, 2]$, and $\beta_{10} = 0.55$. We thus approximate the original model provided in [23] for C-rates between 0.5 and 2 using linear interpolation. The higher capacity fade caused by lower C-rates may result from the effect of superimposed capacity fade caused by pure cycle and calendar aging: Low C-rate cycles cause longer battery utilization for achieving the same amount of charge throughput. Based on Eq. 4, one can again obtain the battery charge throughput that would lead to a certain capacity fade, given a certain core temperature. For completeness, we provide the corresponding formula in Eq. 5.

$$Ah_{cyc}(f, T_s, r_c) = \\ 2 \cdot (f/(\beta_8(r_c) \cdot \exp(-\beta_9(r_c)/(R_{gas} \cdot (T_s + \kappa_T)))))^{1/\beta_{10}} \tag{5}$$

Figs. 1(b) and 1(c) show plots of the semi-empirical models for calendar and cycle aging depending on temperature fitted to the data found in references [22] and [23]. We anticipate a superposition principle of calendar and cycle aging for the deterioration of the battery cells [24].

C. State/Action-Based Cell Deterioration

We combine the electro-thermal and lifetime models described above to obtain a state-dependent expression for the deterioration of a battery cell when (dis)charging it at power p for a duration of d starting in state $\mathbf{S}$, denoted by $u(\mathbf{S}, p, d)$. To obtain the actual variable cost incurred, we multiply the deterioration value u by the number of battery cells n times the actual cost per cell c_c. In the following, we denote value x contained in tuple $\mathbf{Y}$ by $\mathbf{Y}.x$.

Fig. 3 provides the algorithm used to compute function $u(\mathbf{S}, p, d)$. It either returns the loss of life fraction u if the

control p is feasible within the specified minimum and maximum states of charge, $SOC_{\min}$ and $SOC_{\max}$, or ∞ otherwise.

In the algorithm listing shown in Fig. 3, k controls the time resolution, e.g., $k = 3600$ would result in one second simulation time increments. The constant γ denotes the month to hours factor $30.5 \times 24 = 732$. The capacity threshold f_{EOL} defines the decommissioning capacity fade, which is set to 20%, i.e., Li-Ion cells would be replaced when they have lost 20% of their nominal energy capacity. We used the algorithm for computing $u(\mathbf{S}, p, d)$ in an efficient search routine to find the maximum charging and discharging power of a cell during the next d hours when starting in state $\mathbf{S}$ and assuming the maximum C-rate of r_c for charging and discharging. We denote the corresponding function by $p_{\max\,/\,\min}(\mathbf{S}, d)$.

IV. Three Dispatch Strategies

Before describing the three dispatch strategies studied in this work in detail, we shortly outline secondary control reserve auctions and our methodology to estimate the per step cost savings and cost of energy storage from a system operator's point of view.

A. Secondary Control Reserve and Battery Economic Value

In the studied context, BES can yield cost savings by providing reserve below market prices. In general, reserve market prices can be determined using a unique price or a pay-as-bid auction mechanism. Price determination differs from region to region, e.g., most reserve markets in the U.S. apply a unique price auction, whereas pay-as-bid auctions are used in several European countries, including Germany. In Germany, it is common to reimburse capacity allowance (EUR/MW) and energy delivery (EUR/MWh) separately. The first compensates for the provision of the offered power in the corresponding time interval, whereas the second compensates for the energy actually delivered. After the tendering, the system operator sorts the offers by capacity fees and accepts bids until it reaches the required amount of reserve power. The accepted bids are then sorted in increasing order by energy price to create a merit order curve, which is used to activate the respective operators according to the current demand.

In this paper, we introduce a cost savings formula that is sufficiently general to model pay-as-bid reserve markets, and thereafter show its application and results for the German market based on historical market data. We consider a scenario where the system operator reduces its ancillary services sourcing costs by deploying BES, i.e., BES is only used when it can provide these services at a lower cost than the prices at which other providers offer it at a given time. Since the market for secondary reserve in Germany is a pay-as-bid market, the supply curve remains disaggregated, i.e., the bids of single providers remain transparent and are not affected by the system operator's dispatch of the battery energy storage. The total cost savings that can be obtained by the battery are thus equal to the avoided reserve sourcing costs of the system operator minus the BES usage cost.

B. System Operator Cost Savings Obtained from Energy Storage

We compare three strategies for dispatching an energy storage consisting of LiBs providing reserve: a naive (NAI) approach, a one-step cost minimization (OSM) approach, and a probabilistic two-step cost minimization (TSM) approach. The three presented dispatch strategies differ in the amount of information about the relevant environment they leverage. This information includes battery state, battery characteristics including cell aging and corresponding variable usage costs, market prices, as well as statistical information on reserve activation. Each strategy is able to provide a *feasible* dispatch p_t for storage dispatch in subsequent time intervals t of duration d_c hours. By feasible dispatch we mean a value within the maximum (dis)charging capability returned by $p_{\max\,/\,\min}(\mathbf{S}_t, d_c)$. Furthermore, all dispatch strategies make sure that the storage does not lead to higher reserve requirements than the tendered amount.

At any time, there exist two separate bid curves for positive and negative reserve, i.e., we have to distinguish two cost savings functions. We denote the cost savings that can be obtained by the energy storage during the time interval starting at time t and lasting for d_c hours if the dispatch is p_t by $\mathfrak{R}(p_{r,t}, p_t)$, where $p_{r,t}$ is the activated reserve power in time interval $[t, t + d_c]$. The dispatch value p_t refers to cell power, which translates to grid-side power by scaling with the number of cells n and considering power electronics efficiency η. The storage cost savings function is formally defined in Eq. 6 below.

$$\mathfrak{R}(p_{r,t}, p_t) = \int_{x=p_{r,t}}^{p_{r,t}-\min[0,n\cdot p_t/\eta]} d_c \cdot \mathfrak{P}_{r,t}^{\mathrm{neg}}(x) \cdot x \mathrm{d}x \tag{6a}$$

$$+ \int_{x=p_{r,t}-\max[0,n\cdot\eta\cdot p_t]}^{p_{r,t}} d_c \cdot \mathfrak{P}_{r,t}^{pos}(x) \cdot x \mathrm{d}x \tag{6b}$$

Eq. 6a describes the cost reduction that can be achieved if the storage delivers negative reserve, i.e., if the battery is charged. The second part, 6b, describes the cost reduction achieved by providing positive reserve, i.e., if the battery is discharged. Functions $\mathfrak{P}_{r,t}^{\mathrm{neg}}(p)$ and $\mathfrak{P}_{r,t}^{pos}(p)$ yield the marginal reserve energy prices in EUR/MWh when activating an amount of p MWs of negative or positive reserve during time interval $[t, t + d_c]$, respectively. The integrals of Eqs. 6 therefore express the system operator's variable reserve cost. In a pay-as-bid context, the price functions $\mathfrak{P}_t^{pos/neg}(x)$ are increasing, in a unique price context prices only vary with t.

C. Naive Dispatch (NAI)

The naive dispatch strategy only uses the battery model to compute the minimum and maximum grid power in subsequent dispatch intervals. It then dispatches the storage to cover as much of the activated reserve in that time interval as possible. Thus, if positive reserve is required, i.e., $p_{r,t} > 0$, it delivers $p_t^{NAI} = \min[n \cdot \eta \cdot p_{\max}(\mathbf{S}_t, d_c), p_{r,t}]$. If negative reserve is required, it delivers $p_t^{NAI} = \max[n \cdot p_{\min}(\mathbf{S}_t, d_c)/\eta, p_{r,t}]$.

D. One-Step Cost Minimization (OSM)

The one step cost minimization strategy considers the variable cost savings that can result from delivering different amounts of reserve in the current time period, as well as the corresponding usage cost based on the battery life time models described in Section III-B. In the following, we denote the overall cost savings achieved during period $[t, t+d_c]$ by $\Pi(\mathbf{S}_t, p_{r,t}, p_t)$. It is defined formally in Eq. 7 below.

$$\Pi(\mathbf{S}_t, p_{r,t}, p_t) = \mathfrak{R}(p_{r,t}, p_t) - n \cdot c_c \cdot u(\mathbf{S}_t, p_t, d_c) \quad (7)$$

The corresponding optimization problem is defined in Eq. 8. We denote the resulting dispatch by $p^{OSM}(\mathbf{S}_t, p_{r,t})$.

$$\max_{p_t} \quad \Pi(\mathbf{S}_t, p_{r,t}, p_t) \quad (8a)$$

$$\text{s.t.} \quad p_{min}(\mathbf{S}_t, d_c) \leq p_t \leq p_{max}(\mathbf{S}_t, d_c) \quad (8b)$$

$$p_{r,t} + n \cdot p_t \cdot \eta \geq p_{r,t}^{min} \quad (8c)$$

$$p_{r,t} + n \cdot p_t / \eta \leq p_{r,t}^{max} \quad (8d)$$

Eq. 8a is the goal function describing the actual cost savings in the current dispatch interval, i.e., the market cost savings minus the total storage usage cost. Eq. 8b is a constraint making sure that the dispatch is feasible, i.e., that it neither leads to SOCs below or above the specified SOC range, nor exceeds the maximum C-rate. Eqs. 8c and 8d make sure that the power generated or consumed by the energy storage never creates a new peak of required negative or positive reserve. The maximum reserve power values $p_{r,t}^{\min} < 0$ and $p_{r,t}^{\max} > 0$ are known ex-ante.

The advantage of this dispatch strategy is that it compares cost savings potential with usage cost in every dispatch interval, i.e., it leverages more information than the naive dispatch strategy. It will only use the storage if the corresponding cost savings are greater than the cost in the current time step. This leads to a highly risk-averse behavior that does not take long-term effects into account. In particular, the disadvantage of this short-sighted behavior is the potential loss of high future cost saving opportunities at the expense of incurring minor costs in the current time step. For instance, an empty energy storage could miss the chance to deliver highly lucrative positive reserve when not charging during times of low marginal prices for negative reserve, and vice versa.

E. Probabilistic Two-Step Cost Minimization (TSM)

The idea of the probabilistic two-step dispatch strategy is to improve one-step cost minimization by also taking future opportunities for cost saving into account. Accurate predictions of reserve activation amounts in future time intervals are hard since they result from unpredictable random processes such as generator failures and inaccuracies of demand and renewable energy supply forecasts. The variability of reserve demand time series is very high and they are not subject to any seasonality. However, as we show in the following, the overall distribution of the demand for reserve can still be used to inform a dispatch strategy.

The two-step dispatch strategy trades off the secure cost savings that can be achieved in the current time step against the expected cost savings in the following dispatch period. A common notion from inventory management is an optimal inventory level, i.e., the amount of inventory that would maximize profits based on expected demand. We transfer this notion to our setting, i.e., we calculate the optimal state of charge of the energy storage provided the probability that a certain demand for reserve materializes in the next time step. From this maximum expected cost saving we subtract the expected costs saved of the state the storage transitions to according to the dispatch applied at the current time step. We denote the probability density function of reserve demand by $\phi(x)$ in the following. Eqs. 9 provide the full optimization problem to be solved.

$$\max_{p_t} \quad \Pi(\mathbf{S}_t, p_{r,t}, p_t) \quad (9a)$$

$$+ \max_{s} \int_{x=p_{r,t+d_c}^{\min}}^{p_{r,t+d_c}^{\max}} \phi(x)\Pi(\mathbf{S}(s), x, p^{OSM}(\mathbf{S}(s), x))\mathrm{d}x \quad (9b)$$

$$- \int_{x=p_{r,t+d_c}^{\min}}^{p_{r,t+d_c}^{\max}} \phi(x)\Pi(\mathbf{S}_{t+d_c}, x, p^{OSM}(\mathbf{S}_{t+d_c}, x))\mathrm{d}x \quad (9c)$$

$$\text{s.t.} \quad p_{\min}(\mathbf{S}_t, d_c) \leq p_t \leq p_{\max}(\mathbf{S}_t, d_c) \quad (9d)$$

$$\mathbf{S}_{t+d_c} = nextState_p(\mathbf{S}_t, p_t, d_c) \quad (9e)$$

$$\mathbf{S}_{t+d_c} \neg invalid \quad (9f)$$

$$\mathbf{S}(s) = [\mathbf{S}_{t+d_c}.f, s, \mathbf{S}_{t+d_c}.T_c, \mathbf{S}_{t+d_c}.T_s] \quad (9g)$$

$$p_{r,t} + n \cdot p_t \cdot \eta \geq p_{r,t}^{\min} \quad (9h)$$

$$p_{r,t} + n \cdot p_t / \eta \leq p_{r,t}^{\max} \quad (9i)$$

Eq. 9a describes the one-step cost savings that can be achieved with certainty. Eq. 9b yields the maximum expected cost savings in the next time step, i.e., if the storage transitioned to the optimal SOC. Eq. 9c describes the cost savings that can be expected if dispatch p_t is applied in the current dispatch interval. In Eq. 9b and 9c, the expression $p^{OSM}(.,.)$ inlines the one-step optimization problem provided by Eqs. (8), i.e., expected cost savings are computed by summing up the products of optimal cost savings and their corresponding probabilities.

Constraint 9d makes sure that the first step dispatch is feasible with respect to allowed SOC and C-rate ranges. Constraints 9e and 9f model the state evolution and make sure that the dispatch in the second step is feasible. The function $nextState_p$ computes the next state based on the current state, the desired power level, and the duration d. Its algorithm is provided in Fig. 4.

Eqs. 9g and 9h make sure that the power generated or consumed by the energy storage in the first step never creates a new peak of required negative or positive reserve. The corresponding requirement for the second step is implicitly accounted for by our use of expression $p^{OSM}(.,.)$.

```
Input: S, p, d
for t = 1 → k · d do
    if p = 0 then
        I ← 0
    else
        I ← getI(S, p)
        if |I| > r_c · CAP_c then
            S ← invalid
            return S
    S ← nextState_I(S, I, d/k)
    if S.SOC < SOC_min or S.SOC > SOC_max then
        S ← invalid
        return S
return S
```

Fig. 4. Algorithm for computing value of $nextState_p(\mathbf{S}, p, d)$.

V. Simulation Study

To evaluate the proposed dispatch strategies, we conducted a set of experiments using two years worth of German secondary reserve demand (2012 and 2013) and the corresponding price curves. Secondary reserve is dispatched in 15 minutes long intervals in Germany, i.e., our study is based on a trace of $2 \times 365 \times 24 \times 4 = 70,080$ values describing the demand for secondary reserve energy over the course of two years. In Germany, four pay-as-bid auctions for pricing reserve energy are conducted every week. Two are for pricing positive reserve, one of them for time intervals between 8 a.m. and 8 p.m. on weekdays ("main" time), and another one for time intervals on weekdays from 8 p.m. to 8 a.m. and on weekends ("ancillary" time). The remaining two auctions are for pricing negative reserve, with the same distinction between time intervals. For two years, this results in $4 \times 106 = 424$ price curves. The actual payments from the operator to the reserve providers can be derived from the price curves shown in Fig. 5(a) and the demand for reserve during a given 15 minutes long time interval shown in Fig. 5(b). Prices are thus highly variable over time.

Fig. 5(a) shows a plot of all 424 reserve energy price curves, i.e., the outcomes of all auctions carried out in 2012 and 2013. These price curves reveal that the system operator can often save more reserve activation cost per MWh if it charges the energy storage during peaks of negative reserve demand compared to providing positive reserve by discharging the energy storage. However, providing positive reserve would also result in savings when demand is smaller, whereas prices for negative reserve only become greater than zero when more than 1 GW of negative reserve is required.

Fig. 5(b) shows a three day long excerpt of the reserve demand time series indicating its high variance and missing trends. Fig. 5(c) provides a normalized histogram of the entire data set as well as the fitted probability function $\phi(.)$, which we approximated using a Gaussian kernel density estimator. The empirical maximum of negative reserve required in 2012/13 is $p_{r,t}^{\min} = -2245.5$ MW during main time, and $p_{r,t}^{\min} = -2233.6$ MW during ancillary time. The maximum positive reserve requirement was $p_{r,t}^{\max} = 2122.8$ MW during main time, and $p_{r,t}^{\max} = 2099.6$ MW during ancillary time.

A. Setup and Implementation

To evaluate the impact of different parameter configurations on the system operator's cost savings from using the lithium-ion based energy storage to deliver reserve energy, we have carried out several experiments using actual data (activated reserve and price curves) described above and specific parameters required to fully parametrize the battery model. These parameters include nominal energy storage capacity, allowed SOC and C-rate ranges, cell cost, and the applied dispatch strategy. The properties of the considered LFP cell are provided above. We consider a SOC range of $[0.05, 0.95]$ and maximum C-rates equal to 1 and 2 C, respectively. The cell cost is a sensitivity parameter with great impact to the overall cost calculations shown in the following sections. Detailed analysis on Li-Ion battery pack cost is available for automotive packs, but reliable data for stationary storage is scarce [4]. We consider a battery price range of $c_b = 600$ EUR/kWh up to 800 EUR/kWh. We obtain the cost per cell according to $c_c = c_b \cdot E_c$, where $E_c = V_{nom} \cdot CAP_c$ is the nominal energy capacity of one battery cell.

We approximate n based on the required nominal capacity of the energy storage, E_b, using $n = \lceil E_b/E_c \rceil$. To keep the computational complexity of running the simulations within acceptable limits, we precompute the cell cost function $u(\mathbf{S}, p, d)$. We do this by computing its output for discrete combinations of the input parameters, in particular, r_c, f, SOC, T_c, T_s, and p, and applying linear interpolation to obtain continuous values.[1] Interpolated values are only used for optimization, not for evaluation.

During simulation, dispatch values, according to the selected storage operation strategy, are computed before each dispatch interval lasting 15 minutes. Battery cell states are then simulated during each interval at 1 s time resolution. When capacity fade reaches the end-of-life level (20%), it is set back to zero with no additional cost.

B. Results

Fig. 6 reveals how selected behavioral metrics and obtained per-step cost savings evolve depending on the applied BES dispatch strategy. Fig. 6(a) shows a cumulative duration curve of all SOCs. We use cumulative duration curves because crucial differences would otherwise not be visible on the plots. The different dispatch strategies result in significantly different SOC dwell times. In particular, TSM dispatch results in a more complex SOC dwell time pattern than NAI and OSM dispatch, indicating its ability to evaluate the cost savings potential of a certain SOC level in addition to the cost savings resulting from immediate dispatch decisions.

Fig. 6(b) shows the expected impact of greedy battery usage on capacity fade: Higher battery utilization leads to significantly faster aging, whereas C-rate does not have a major impact.

Fig. 6(c), which shows the cumulative distribution of BES power levels observed over time, indicates that the storage system only operates in charge/discharge mode during 40% of the time, irrespective of the chosen dispatch strategy. Furthermore,

[1]The accuracy of the chosen interpolation method depends on the respective variable increments used. We tuned these increments until the accuracy of the interpolation was higher than 99.9%. It has turned out that some of the parameters have a less significant impact on the accuracy of the interpolation under the given circumstances, which helps to reduce the parameter space.

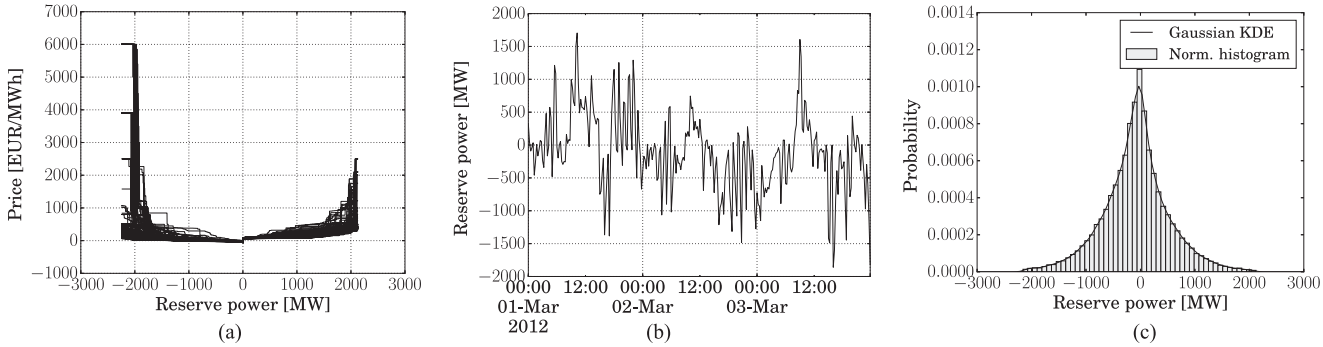

Fig. 5. Input data for simulation. (a) Secondary reserve prices (424 price curves). (b) Activated secondary reserve (3 days). (c) Probability of reserve activation (2 years).

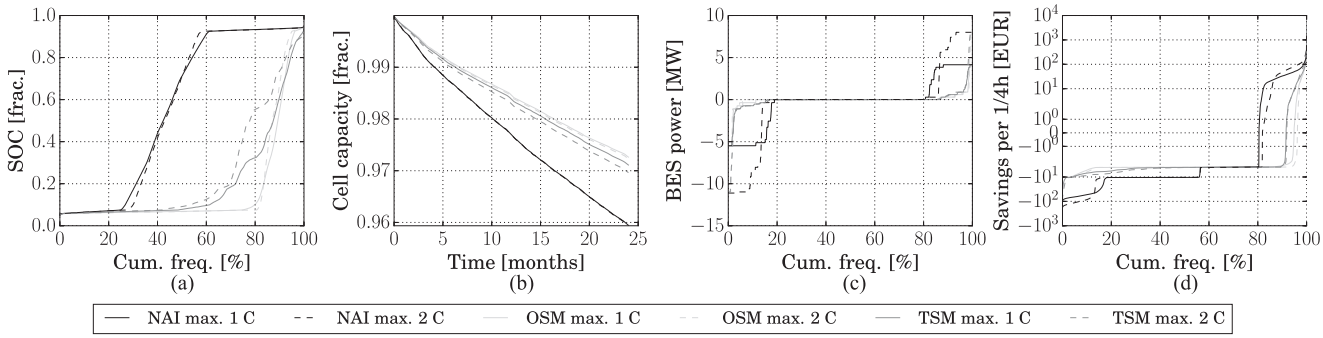

Fig. 6. Storage operation statistics ($E_s = 5$ WMh, $c_b = 800$ EUR/kWh). (a) SOC distribution. (b) Capacity fade. (c) Power distribution. (d) Savings distribution.

this plot shows that the naive dispatch strategy leads to a much greater energy throughput than the cost-based strategies, which explains the greater battery wear.

Fig. 6(d) shows the per step cost savings measured on a logarithmic scale. It reveals that the naive strategy produces both, greater cost savings and greater cost increases, compared to the other strategies. In contrast, the OSM strategy never causes losses exceeding the cost of zero dispatch, which equals calendar aging cost. The TSM strategy outperforms the OSM strategy in the very high cost savings range due to its ability to probabilistically gauge future cost saving opportunities.

Fig. 7 (shows plots of the *average cost savings per MWh of nominal BES capacity per day* for different storage capacities, C-rates, and battery cost levels. This unit makes cost savings comparable across parameter configurations and could be used in corresponding investment studies.

Figs. 7(a) and (b) show cost savings at a conservative battery price of $c_b = 800$ EUR/kWh. They indicate a clear advantage of the OSM and TSM strategies over the naive dispatch. Naive BES dispatch leads to significant losses, which become even more pronounced if one allows for battery operation at higher C-rates. In contrast to this, the OSM and TSM strategies are not significantly affected by variations of C-rates since they take the effect of power rate on cost savings explicitly into account. As Fig. 6(a) shows, OSM keeps SOC levels low during most of the time, although it does not inherently consider the long-term advantage of this behavior in terms of calendar aging (cf. Fig. 1(b)). In contrast, the TSM dispatch strategy explicitly takes the battery deterioration cost caused by calendar aging at different SOC levels into account.

Not surprisingly, reducing battery cell costs increases cost savings across all storage operation strategies. Furthermore, the absolute financial advantage of TSM and OSM compared to the naive dispatch decrease, but the expected ranking stays the same. Finally, the chosen capacity range of 5–80 MWh is sufficient to reveal the decreasing marginal returns of additional energy storage capacity, which is to be expected given the shape of the reserve price curves shown in Fig. 5(a) and the way the modeled BES delivers reserve energy.

VI. Discussion

This paper contributes an new approach for cost-minimizing operational dispatch of BES in applications subject to very high variability and uncertainty. Although the relatively high detail and resulting computational complexity of the LiB model discourage its use in long-term planning studies, it could still be used to inform such studies, e.g., by comparing the long-term aging effect of different usage features and limits.

We investigate the use case of providing secondary control reserve, which cannot be predicted sufficiently well to apply prediction-based methods like Model Predictive Control (MPC). The probabilistic two-step cost minimization method we presented in Section IV-E differs from MPC as it uses the distribution of historical reserve demand directly instead of predicting

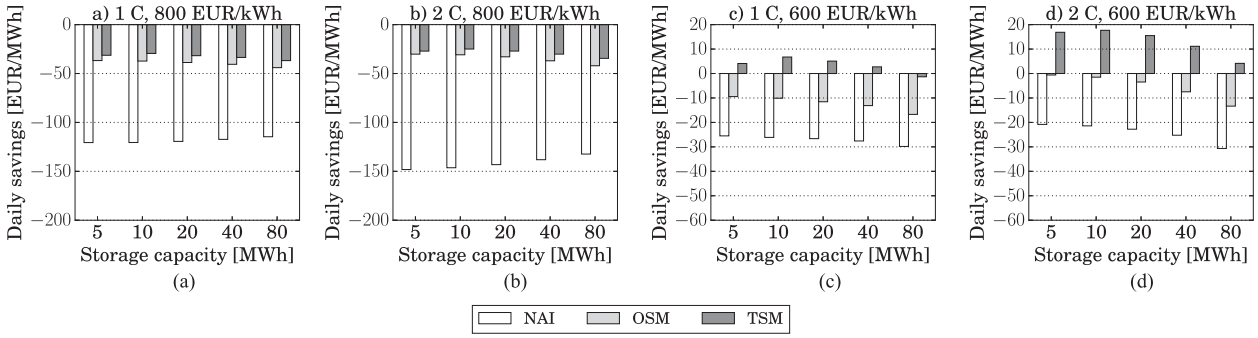

Fig. 7. Cost savings for different nominal energy storage capacities E_s, C-rates r_c, and battery cost c_b.

a trajectory of future values.[2] Although we test our method using German data, our method can be applied in any jurisdiction where a financial valuation of provided control reserve exists, including other European countries and the US. It should also be mentioned that the methods we propose can be applied to any spot valued product, including other ancillary services, energy traded on spot markets (i.e., day-ahead and intra-day markets), as well as combinations thereof.

The electro-thermal battery cell model we use is more detailed than the models used in the related literature and enables the use of existing semi-empirical battery aging models. Our contribution is among the first to consider battery cost as variable term that can be directly compared to short-term cost saving opportunities. An important limitation regarding our cell model is that it only predicts the behavior of state-of-the-art LFP cells, i.e., it would require additional parameter fitting to be applied to other lithium-ion battery cell chemistries.

Regarding solving time, it is important to understand that we are able to pre-compute the simulated battery cell aging. From an operational point of view, the pre-computation part is not time-critical because it only needs to be done once and can be executed offline. The actual use of the pre-computed models then reduces to a basic one-dimensional search, which can be carried out within milliseconds. In the case of TSM, the inline optimization problem, whose solution is the expected value of the next state, only needs to be re-computed every time the price functions change, i.e., once per week in our use case. As such, despite this process takes several minutes, TSM inline optimization for the tender does not resemble a crucial constraint either. It is worth mentioning, that in the method demonstration presented herein we prototyped all features in Python. A more efficient implementation (e.g., using C) and parallelization of the search process might allow for further reducing solving time.

Our results presented in Section V-B show that the proposed dispatch strategies work well, even though they do not rely on predictions. In fact, we compare the cost-based dispatch strategies to the naive dispatch previously proposed for symmetrical reserve provision using BES [1], which is already highly effective in this use case. On the one hand, all dispatch approaches proposed in this paper allow for determining LiB capability very accurately, which is especially important in applications that are critical to grid safety, but can also increase battery utilization. In particular, we tested charging and discharging rates of up to 2 C, which exceed typical power ranges assumed in the related literature. On the other hand, state/action-based cost models are a precondition for developing dispatch strategies that explicitly compare financial costs and benefits during battery operation.

In this study, we do not consider NPV, which would require quantification of up-front cost, e.g., for storage periphery, and various financial parameters, such as interest rates. However, as the purpose of this paper is not primarily to investigate BES profitability per se, we do not consider this very informative. After all, battery cell prices, as well as the financial valuation of ancillary services, constantly change. Moreover, as the rather low utilization of the BES in our use case suggests, the profitability of BES investments could be further increased by providing multiple services [25]. Another limitation of this work is the effort required to fit and parametrize the required models. Applying our approach to other battery cell types would thus require significant upfront measurement experiments and statistical expertise if high-quality models do not yet exist.

VII. Conclusion

In this paper, we have demonstrated the potential advantages of using more detailed battery models not just for evaluation, but also for making operational dispatch decisions. The value of these models has been demonstrated in a secondary reserve use case that explicitly considers the unpredictable demand for reserve. We expect that our encouraging results will motivate further research on intelligent, cost-aware battery dispatch strategies. In our opinion, this could accelerate the market entry of battery energy storage for grid-scale applications and thereby help integrating variable renewable energy more efficiently.

[2]Model Predictive Control (MPC) is based on the idea of predicting the evolution of relevant system variables until a specified time horizon at each control step, optimizing the control variables until that time, and then implementing the control(s) in the first time step only.

References

[1] T. Borsche, A. Ulbig, M. Koller, and G. Andersson, "Power and energy capacity requirements of storages providing frequency control reserves," in *Proc. IEEE PES General Meeting*, Jul. 2013, pp. 1–5.

[2] P. Ribeiro, B. Johnson, M. Crow, A. Arsoy, and Y. Liu, "Energy storage systems for advanced power applications," *Proc. IEEE*, vol. 89, no. 12, pp. 1744–1756, Dec. 2001.

[3] Younicos, "Schwerin battery park." [Online]. Available: http://www.younicos.com/download/Younicos_Reference_Project_Schwerin_EUR_Web.pdf, Oct. 2014, accessed: Oct. 30, 2015.
[4] B. Nykvist and M. Nilsson, "Rapidly falling costs of battery packs for electric vehicles," *Nature Climate Change*, vol. 5, pp. 329–332, Mar. 2015.
[5] B. Dunn, H. Kamath, and J.-M. Tarascon, "Electrical energy storage for the grid: A battery of choices," *Science*, vol. 334, no. 6058, pp. 928–935, Nov. 2011.
[6] H. Mohsenian-Rad, "Optimal bidding, scheduling, and deployment of battery systems in california day-ahead energy market," *IEEE Trans. Power Syst.*, vol. 31, no. 1, pp. 442–453, Jan. 2016.
[7] N. Li, C. Uckun, E. Constantinescu, J. Birge, K. Hedman, and A. Botterud, "Flexible operation of batteries in power system scheduling with renewable energy," *IEEE Trans. Sustain. Energy*, vol. 7, no. 2, pp. 685–696, Apr. 2016.
[8] I. Duggal and B. Venkatesh, "Short-term scheduling of thermal generators and battery storage with depth of discharge-based cost model," *IEEE Trans. Power Syst.*, vol. 30, no. 4, pp. 2110–2118, Jul. 2015.
[9] R. L. Fares and M. E. Webber, "A flexible model for economic operational management of grid battery energy storage," *Energy*, vol. 78, pp. 768–776, Dec. 2014.
[10] M. A. Ortega-Vazquez, "Optimal scheduling of electric vehicle charging and vehicle-to-grid services at household level including battery degradation and price uncertainty," *IET Gener., Transm. Distrib.*, vol. 8, no. 6, pp. 1007–1016, Jun. 2014.
[11] J. Li and M. A. Danzer, "Optimal charge control strategies for stationary photovoltaic battery systems," *J. Power Sources*, vol. 258, pp. 365–373, Jul. 2014.
[12] M. Koller, T. Borsche, A. Ulbig, and G. Andersson, "Defining a degradation cost function for optimal control of a battery energy storage system," in *Proc. IEEE PowerTech*, Jun. 2013, pp. 1–6.
[13] S. Teleke, M. Baran, S. Bhattacharya, and A. Huang, "Optimal control of battery energy storage for wind farm dispatching," *IEEE Trans. Energy Convers.*, vol. 25, no. 3, pp. 787–794, Jun. 2010.
[14] C. Goebel and H. A. Jacobsen, "Bringing distributed energy storage to market," *IEEE Trans. Power Syst.*, vol. 31, no. 1, pp. 173–186, Jan. 2016.
[15] N. Lu, M. Weimar, Y. Makarov, and C. Loutan, "An evaluation of the NaS battery storage potential for providing regulation service in California," in *Proc. IEEE/PES Power Syst. Conf. Expo.*, Mar. 2011, pp. 1–9.
[16] P. Mercier, R. Cherkaoui, and A. Oudalov, "Optimizing a battery energy storage system for frequency control application in an isolated power system," *IEEE Trans. Power Syst.*, vol. 24, no. 3, pp. 1469–1477, Aug. 2009.
[17] A. Oudalov, D. Chartouni, and C. Ohler, "Optimizing a battery energy storage system for primary frequency control," *IEEE Trans. Power Syst.*, vol. 22, no. 3, pp. 1259–1266, Aug. 2007.
[18] C. Lu, C. Liu, and C. Wu, "Dynamic modelling of battery energy storage system and application to power system stability," *IEE Proc.—Gener., Transm. Distrib.*, vol. 142, no. 4, pp. 429–435, Aug. 1995.
[19] X. Lin *et al.*, "A lumped-parameter electro-thermal model for cylindrical batteries," *J. Power Sources*, vol. 257, pp. 1–11, Jul. 2014.
[20] M. R. Jongerden and B. R. Haverkort, "Battery Modeling," Tech. Rep. TR-CTIT-08-01, Center for Telematics and Inf. Technol., Univ. Twente, Enschede, The Netherlands, 2008.
[21] C. Weng, J. Sun, and H. Peng, "An open-circuit-voltage model of lithium-Ion batteries for effective incremental capacity analysis," in *Proc. ASME Dyn. Syst. Control Conf.*, Oct. 2013, pp. V001T05A002–V001T05A002.
[22] M. Swierczynski, D.-I. Stroe, A.-I. Stan, R. Teodorescu, and S. Kaer, "Lifetime estimation of the nanophosphate LiFePO4/C battery chemistry used in fully electric vehicles," *IEEE Trans. Ind. Appl.*, vol. 51, no. 4, pp. 3453–3461, Jul.–Aug. 2015.
[23] J. Wang *et al.*, "Cycle-life model for graphite-liFePO4 cells," *J. Power Sources*, vol. 196, no. 8, pp. 3942–3948, Apr. 2011.
[24] S. Schuster *et al.*, "Nonlinear aging characteristics of lithium-Ion cells under different operational conditions," *J. Energy Storage*, vol. 1, pp. 44–53, May 2015.
[25] O. Mégel, J. L. Mathieu, and G. Andersson, "Scheduling distributed energy storage units to provide multiple services," in *Proc. Power Syst. Comput. Conf.*, Nov. 2014, pp. 1–7.

Christoph Goebel (M'12) received the diploma degree in information engineering and management from Karlsruhe Institute of Technology, Karlsruhe, Germany, in 2006 and the doctorate degree in information systems from Humboldt University Berlin, Berlin, Germany, in 2009. Until his graduation, he spent one year studying computer science at the Swiss Federal Institute of Technology, Lausanne, and half a year at Carnegie Mellon University, Pittsburgh, PA, USA. After completing his dissertation, he worked as a Postdoctoral Fellow at the University of California, Berkeley, CA, USA, for 1.5 years. In Berkeley, he started research in the area of sustainable energy management. Until April 2016, he worked as an Assistant Professor at the Department of Computer Science, Technical University Munich, Munich, Germany. His current research interests are in the area of using information technology 1) to facilitate renewable integration with flexible loads and distributed energy storage and 2) to improve energy efficiency in different contexts, e.g., buildings.

Holger Hesse received the M.Sc. and Ph.D. degrees in physics from the Ludwig Maximilian University of Munich, Munich, Germany and conducted interdisciplinary research at the University of Wollongong, Wollongong, Australia. After his graduation, he worked at Bertrandt AG as a Project Lead Engineer and R&D consultant in the field of electric vehicle and lithium-ion battery storage development. Since 2014, he has been with Technical University Munich's Institute for Electrical Energy Storage Technology, Munich, Germany, leading the research group on stationary energy storage. His research focuses on the technical challenges and economic opportunities when bringing stationary energy storage in on-grid and off-grid applications.

Michael Schimpe received the M.Sc. degree in mechanical engineering, after studies in Munich and Singapore, from the Technical University of Munich, Munich, Germany, in 2014. Before his graduation, he gained industry experience at BMW, Linde, and Siemens in the field of renewable energy and energy storage. He now continues at the Technical University of Munich working as a Research Associate at the Institute for Electrical Energy Storage Technology. In his work, he focuses on the system simulation of stationary large-scale battery storage systems.

Andreas Jossen received the diploma degree and doctoral degree in electrical engineering from the University of Stuttgart, Germany, in 1989 and 1994, respectively. From 1994 to 2010, he was with the Centre for Solar Energy and Hydrogen Research, Ulm, Germany, where he was a leader of the battery system technology group. Since 2010, he has been a full Professor at the Technical University of Munich, Germany. He is the founder and head of the Institute for Electrical Energy Storage Technology, Munich, Germany. His research activities are modeling, simulation, and characterization of rechargeable batteries, as well as fundamental and applied topics in battery systems, such as battery topologies, state determination, and control of battery systems.

Hans-Arno Jacobsen (M'96–SM'08) received the doctorate degree in Germany, France, and the USA. He was engaged in postdoctoral research at INRIA near Paris before moving to the University of Toronto in 2001. He was a Professor in the Department of Electrical and Computer Engineering and the Department of Computer Science, University of Toronto, Toronto, ON, Canada. He has conducted pioneering research that lies at the interface between computer science, computer engineering, and information systems. He holds numerous patents and was involved in important industrial developments with partners like Bell Canada, Computer Associates, IBM, Yahoo!, and Sun Microsystems. His principal areas of research include the design and the development of middleware systems, event processing, service computing, and applications in enterprise data processing. His applied research is focused on ICT for energy management and energy efficiency. He also explores the integration of modern hardware components, such as FPGAs (Field Programmable Gate Arrays), into middleware architectures. In 2011, he received the prestigious Alexander von Humboldt-Professorship to direct research at TUM.